ELSEVIER

Journal of Organometallic Chemistry 648 (2002) 72–80

Journal of Organometallic Chemistry

www.elsevier.com/locate/jorganchem

Synthesis and properties of homoannularly- and heteroannularly carbonyl-bridged binuclear ruthenocene derivatives

Masaru Sato *, Masaki Suzuki, Masanori Okoshi, Masaki Kurasina, Masanobu Watanabe

Chemical Analysis Center, Saitama University, Urawa, Saitama 338-8570, Japan

Received 25 June 2001; received in revised form 17 September 2001; accepted 9 October 2001

Abstract

1-Carboxyl-1′,2′,3′,4′,5′-pentamethylruthenocene was heated with $(CF_3CO)_2O$ overnight at 90 °C to give *anti*-8,9,10,11,12,20,21,22,23,24-decamethyl[1.1](2,18)(6,14)ruthenocenophan-1,13-dione in 52% yield, whose structure was determined by X-ray diffraction (XRD). Chlorocarbonylruthenocene was treated with anhydrous aluminum chloride in refluxing dichloroethane to give anti-[1.1](2,18)(6,14)ruthenocenophan-1,13-dione and [1,1](2,20)(6,14)ruthenocenophan-1,13-dione, although, with a tiny yield (3%). In the protonated species of two homoannularly bridged ruthenocenophanes the positive charge was partially delocalized. The structure of the protonated species was determined by XRD. [1,1](2,20)(6,14)Ruthenocenophan-1,13-dione was fluxional and the activation energy ($\Delta G^{\neq} = 56.5$ kJ mol^{-1}) of the dynamic process was determined by the VT-method.

Keywords: Ruthenocenophane; Dynamic process; Protonation; Indacen-4,8-dione

1. Introduction

Metallocenes are a noteworthy object of the research in fundamental and applied chemistry even today [1]. Of stable metallocene, ferrocene, ruthenocene, and osmocene, ferrocene derivatives are especially investigated from a variety of viewpoints, for example, functionality materials and catalysts, probably, because ferrocene has a unique structure and shows a stable one-electron redox behavior [2]. Recently, much attention has been also focused in the chemistry of ruthenocene, in particular, in binuclear ruthenocene derivatives. [1.1]-Ruthenocenophane showed quasi-reversible two-electron redox and gave the complex with a Ru–Ru bond in the oxidation [3]. The two-electron oxidation of 1,2-bis(ruthenocenyl)ethylenes afforded the (μ-η^6, η^6-pentafulvadiene)diruthenium complexes [4]. The Ru(II) ruthenocenylacetylide complexes showed two quasi-reversible one-electron waves in the cyclic voltammetry (CV) and caused a unique structural rearrangement in the oxidation [5,6]. The two-electron oxidation of biruthenocene led to the *anti*-(μ-η^6,η^6-fulvalene) diruthenium complex with a novel coordination mode of a fulvalene ligand [7]. These interesting facts stimulate us to investigate binuclear ruthenocene derivatives further. We here report the synthesis and some properties of binuclear ruthenocene derivatives, which are bridged by two carbonyl groups homoannularly or heteroannularly.

2. Results and discussion

2.1. Synthesis, spectra, and molecular structure

1-Formyl-1′,2′,3′,4′,5′-pentamethylruthenocene (**1**) was oxidized with MnO_2 in the presence of KCN in MeOH to give 1-carbomethoxy-1′,2′,3′,4′,5′-pentamethylruthenocene (2) in 80% yield. The hydrolysis of the ester **2** in aqueous 10% KOH solution afforded 1-carboxyl-1′,2′,3′,4′,5′-pentamethylruthenocene (**3**) in 90% yield. The carboxylic acid **3** was heated with $(CF_3CO)_2O$ overnight at 90 °C to give *anti*-8,9,10,11,12,20,21,22,23,24-decamethyl[1.1](2,18)(6,14)-

* Corresponding author. Fax: +81-48-8583707.
E-mail address: msato@cacs.saitama-u.ac.jp (M. Sato).

0022-328X/02/$ - see front matter
PII: S0022-328X(01)01376-6

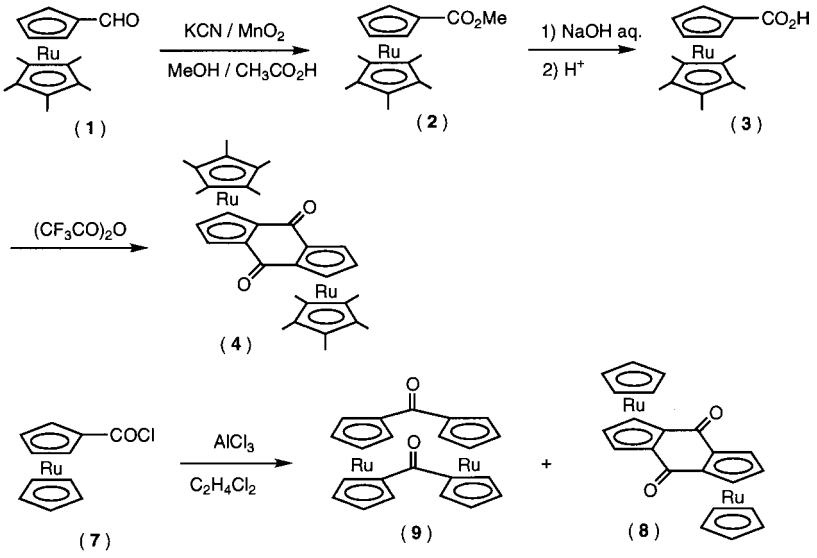

Scheme 1.

ruthenocenophan-1,13-dione (**4**) in 52% yield (Scheme 1). The carbonyl frequency of **4** was observed at 1645 cm^{-1}. The ^{1}H-NMR spectrum of **4** showed the cyclopentadienyl (Cp) ring protons as a triplet (1H) at δ 4.72 and a doublet (2H) at δ 5.02, indicating a symmetrical 1,2-di-substitution of the Cp ring of the ruthenocene moiety. In coincidence with this, only six carbon signals were observed in the ^{13}C-NMR spectrum of **4**. The molecular structure was determined by X-ray diffraction. Half of the molecule of **4** is crystallographically unique, with the whole molecule located on an inversion center. The ORTEP view of **4** is shown in Fig. 1. The crystallographic data are summarized in Table 1 and the selected bond distances and angles are shown in Table 2. The unique feature of **4** is the *anti*-coordination of two (η-C_5Me_5)Ru moieties toward the central indacen-4-dione ligand coordinated by a η^5-coordination mode. This is probably because the Cp* ligand is sterically bulky.

The η-C_5H_3 and η-C_5Me_5 ligands in the pentamethylruthenocenyl parts took an eclipsed conformation and the Ru–C (av. 2.174) and C–C distances (av. 1.424 Å) are typical for ruthenocene derivatives. The central indacen-4-dione ligand is planar and no strain is observed in the bond distances and angles of the frame. As an additional feature, the carbonyl groups in **4** are protected by each one of the methyl groups of the two η-C_5Me_5 ligands in the pentamethylruthenocenyl moiety, because the methyl groups are arranged above and below the plane of carbonyl groups. As a supporting chemical evidence, the reduction of **4** with $LiAlH_4$ or $LiAlH_4$–$AlCl_3$ was tried in various conditions, but **4** never reduced with $LiAlH_4$ or $LiAlH_4$–$AlCl_3$.

Ruthenocene was lithiated with one equivalent of *t*-BuLi in THF at 0 °C and subsequently reacted with ethyl chloroformate to give 1-carbethoxyruthenocene (**5**) and 1,1′-bis(carbethoxy)ruthenocene in 44 and 7.8% yields, respectively. The carboxylic acid (**6**) obtained from the hydrolysis of **5** was treated with $(CF_3CO)_2O$ overnight at 120 °C to give *anti*-[1.1](2,18)(6,14)ruthenocenophan-1,13-dione (**8**) in a tiny yield. The chlorocarbonyl derivative (**7**), which was prepared from **6** and oxalyl chloride in the presence of pyridine, was treated with anhydrous aluminum chloride in refluxing dichloroethane to give diketone **8** in 3% yield, along with [1,1](2,20)(6,14)ruthenocenophane-1,13-dione (**9**) (3%) (Scheme 1). The carbonyl frequency of **8** (1644 cm^{-1}) was observed in the range similar to that of **4**. However, the proton signals (δ 5.01 and 5.48) of the substituted η-C_5H_3 ring and the carbon signal (190.34 ppm) of the carbonyl group of **8** were shifted downfield compared with those of **4**. This is probably, because of

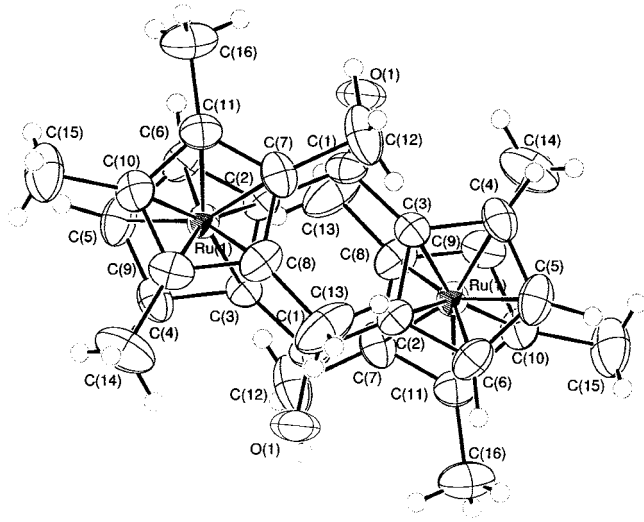

Fig. 1. ORTEP view of compound **4**.

Table 1
Crystallographic data for **4** and **10**

	4	**10**
Molecular formula	$C_{32}H_{36}O_2Ru_2$	$C_{36}H_{36}F_6O_6Ru_2$
Molecular weight	654.78	880.52
Crystal system	Monoclinic	Monoclinic
Space group	$P2_1/c$	$P2_1/a$
a (Å)	11.9130(4)	8.5500(7)
b (Å)	8.1780(4)	26.079(1)
c (Å)	14.8810(6)	8.3950(7)
β (°)	110.902(2)	97.529(4)
V (Å^3)	1353.40(10)	1855.7(2)
Z	2	2
D_{calc} (g cm^{-3})	1.607	1.576
Crystal dimensions (mm)	$0.20\times0.15\times0.16$	$0.4\times0.3\times0.2$
Radiation (λ, Å)	Mo–K_α (0.71073)	Mo–K_α (0.71073)
Reflection (hkl) limits	$-15\le h\le14$, $0\le k\le10$, $0\le l\le19$	$0\le h\le12$, $0\le k\le32$, $-11\le l\le11$
Total reflections measured	2985	5076
Unique reflections	2467	4659
Linear absolute coefficient (mm^{-1})	1.14	8.677
Reflections used in L.S.	2467	3473
L.S. parameters	227	226
R	0.036	0.080
R_w	0.058	0.099
S	1.176	3.549
Max peak in final Fourier map (e Å^{-3})	0.34	1.05
Min peak in final Fourier map (e Å^{-3})	−0.56	−0.94

Table 2
Selected bond distances and bond angles for **4**

Bond distances (Å)			
C(1)–C(2)	1.465(5)	C(2)–C(3)	1.453(5)
C(1)–O(1)	1.221(5)	Ru(1)–C(Cp)	2.184(av.)
Ru(1)–C(Cp*)	2.169(av.)	C–C(Cp)	1.445(av.)
C–C(Cp*)	1.428(av.)		
Bond angles (°)			
C(2)–C(1)–C(3)	113.7(4)	O(1)–C(1)–C(2)	123.3 (4)
O(1)–C(1)–C(3)	123.1(4)	C(1)–C(2)–C(5)	129.3(4)
C(1)–C(2)–C(3)	123.1(4)	C(3)–C(2)–C(6)	107.3 (4)

the presence of the electron-releasing η-C_5Me_5 ligand in **4**.

In the ^{1}H-NMR spectrum of **9**, the signal of the β-ring protons of the ruthenocene moiety is somewhat broadened at room temperature, indicating the presence of a dynamic process. The VT-NMR spectrum of **9** in $CDCl_3$ afforded the α- and β-proton signals as sharp triplets at δ 5.47 and 4.76 at 60 °C. On the other hand, the α-proton signals were observed at δ 5.58 and 5.46 and β-proton signals appeared at δ 4.90 and 4.72 as broad multiplets at −55 °C (Fig. 2). No signal corresponding to an *anti*-isomer was observed, differently from the case of [1,1](2,20)(6,14)ferrocenophane-1,13-dione. The activation free energy for the dynamic process of the fractional molecule **9** was calculated to be $\Delta G^{\neq} = 56.5$ kJ mol^{-1} at 270 K from the coalescence temperature (270 K). The energy is smaller than that of [1,1](2,20)(6,14)ferrocenophane-1,13-dione ($\Delta G^{\neq} = 58.7$ kJ mol^{-1}) [8]. In coincidence with this, the value of $\Delta G^{\neq} = 57.2$ kJ mol^{-1} was reported for the dynamic process of [1,1](2,20)(6,14)ferrocenoruthenocenophane-1,13-dione [9]. It was reported [10] that [1,1]ferrocenophane adopted a *syn*-conformation, having a large flexibility toward a molecular twisting contrary to the *anti*-conformation. Then, the dynamic process observed above seems to be due to a molecular twisting similar to that proposed for *syn*-[1,1]ferrocenophane (Scheme 2). The smaller $\Delta G^{\neq}$ value for [1,1](2,20)(6,14)ruthenocenophane-1,13-dione compared with those for [1,1](2,20)(6,14)ferrocenophane-1,13-dione and [1,1]-(2,20)(6,14)ferrocenoruthenocenophane-1,13-dione seems to reflect the increase of the molecular flexibility, which is caused by the larger interring distance for ruthenocene (3.68 Å) compared with that for ferrocene (3.32 Å).

2.2. Electrochemistry

Diketones **4** and **8** are formally considered to be a quinone fused two ruthenocenes. Therefore, the reduction potentials of compounds **4** and **8**, as well as benzoquinone and anthraquinone, were measured by

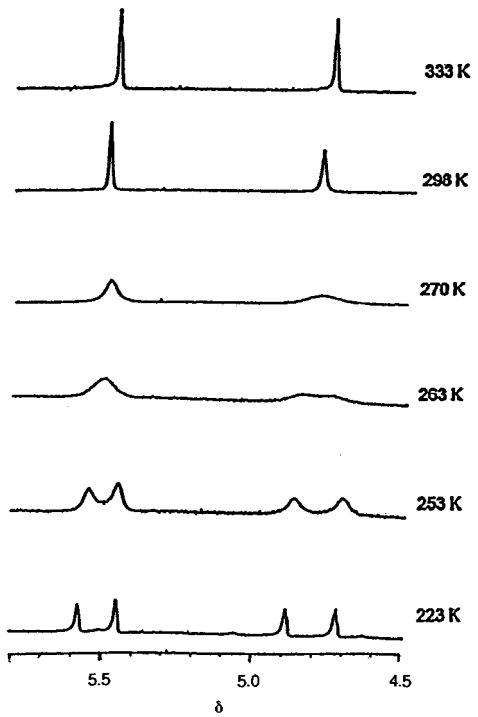

Fig. 2. VT-NMR spectrum of **9**.

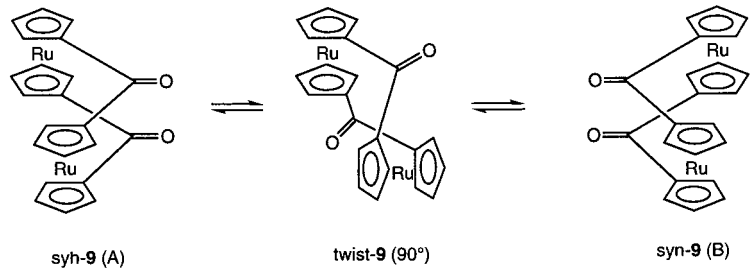

Scheme 2.

cyclic voltammetry (CV) and the reduction potentials were summarized in Table 3. Benzoquinone showed two quasi-reversible redox waves at half wave potential ($E_{1/2}$) = −0.96 and −1.50 V, while anthraquinone showed one broad reduction wave and one broad oxidation wave due to the carbonyl group at E_{pc} = −1.55 V, and E_{pa} = −1.31 V, respectively. On the other hand, diketones **4** and **8** exhibited only one broad reduction wave at E_{pc} = −1.42 and −1.46 V, respectively, (the cyclic voltammograms were broad due to a little solubility of the samples). The fusion of two benzene rings to benzoquinone makes difficult to reduce largely (ΔE_{pc} = 0.50 V), because of the lack of the quinoid character. It is well known that, ruthenocene has an electron-releasing ability similar to ferrocene. So, the fusion of ruthenocene to benzoquinone is expected to increase the difficulty of diketones for reduction compared with the fusion of benzene. However, the reduction potential of **4** (ΔE_{pc} = 0.37 V) and **8** (ΔE_{pc} = 0.41 V) is lower than that of anthraquinone. This may be probably, because, the radical anion forming in reduction of **4** and **8** is stabilized by the delocalization to the Ru metal center as shown in Scheme 3.

2.3. Protonation and methylation

It is well known that a ferrocenyl group strongly stabilizes a α-carbonium cation and a ruthenocenyl group also has a similar ability [11]. So, the carbonyl group of acetylferrocene is much more easily protonated than the metal atom to give the ferrocenyl-stabilized carbocation [12]. Diketones **4** and **8** were dissolved in strong acid to give a violet and brown solution, respectively. In the UV–vis spectrum of **4** and **8** in 60% H_2SO_4, considerably strong absorptions were observed at 554 and 534 nm, respectively. These absorption bands may be probably the MLCT band, which is caused by the delocalization of the positive charge to the metal site due to the canonical structures **A**–**C** as shown in Scheme 4. The bathochromic shift in **4** may be caused by the larger delocalization of the positive charge due to the electron-releasing methyl group compared with **8**. The ^{1}H-NMR spectrum of **4** in CF_3COOD showed the down-field shift of the η-C_5H_3 ring protons (Δδ 0.77 ppm) and the methyl protons (Δδ 0.09 ppm). A similar, but somewhat smaller down-field shift (Δδ 0.56 and 0.62 ppm for the η-C_5H_3 ring and Δδ 0.31 ppm for the η-C_5H_5 ring) was also observed in **8**. These indicate that the positive charge in the protonated cations of **4** and **8** is delocalized to the ruthenocenyl moiety as shown in Scheme 4. However, it is considered that the delocalization is partial and the contribution of the canonical structure **C** is small, because, it was reported that the proton signal of the η-C_5H_5 ring of $[(\eta\text{-}C_5H_5)Ru(\eta^6\text{-}C_5Me_4CH_2)]^+$ was shifted to down-field by 1.0 ppm compared with that of the neutral species [13]. A similar down-field shift (Δ 0.98 ppm) was also observed when ruthenocenylmethanol was dissolved in CF_3COOD. When bis(ruthenocenyl)ketone [14] was dissolved in CF_3COOD, the ^{1}H-NMR spectrum of the protonated species showed the proton signal for the η-C_5H_5 ring at δ 4.87, the α- and β-proton signals for the η-C_5H_4 ring at δ 5.60 and 5.43, respectively. The down-field shift of the former from the corresponding proton signal of the neutral ketone is Δ = 0.29 ppm and those of the latter are Δ = 0.34 and 0.70 ppm, respectively. The value of the down-field shift is nearly similar to those observed in **8**. Therefore, it is considered that the positive charge in the protonated ketones is not delocalized sufficiently to the central metal in the ruthenocene moiety compared with that in the $[(\eta\text{-}C_5H_5)Ru(\eta^6\text{-}C_5Me_4CH_2)]^+$ complex.

The violet solution of **4** in a small amount of CF_3COOH was diffused with pentane to give red crystals (**10**) in high yield. The crystals were moisture-sensitive and turned back to the starting yellow **4** on keeping in the air, gradually even in crystal state. The ^{1}H-NMR

Table 3
Redox potentials of diketones [a]

Comound	E_{pa}(**1**)	E_{pc}(**1**)	E_{pa}(**2**)	E_{pc}(**2**)
Benzoquinone	−0.86	−1.05	−1.40	−1.60
Anthraquinone	−1.31	−1.55		
4		−1.42		
8		−1.46		

[a] Versus $FcH/FcHt^+$.

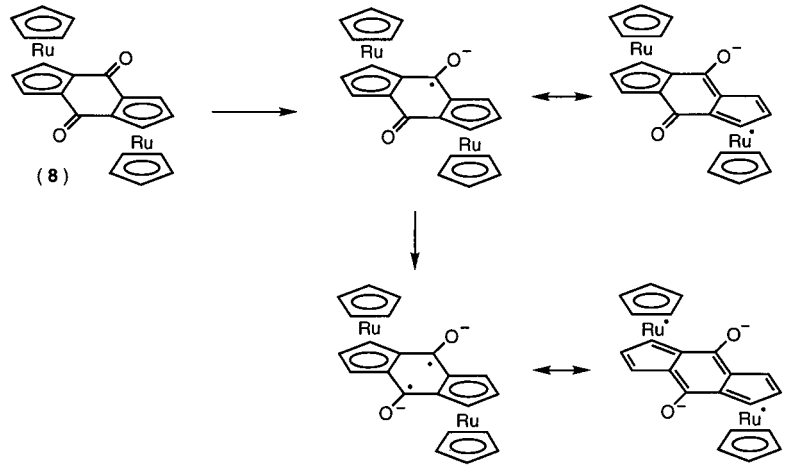

Scheme 3.

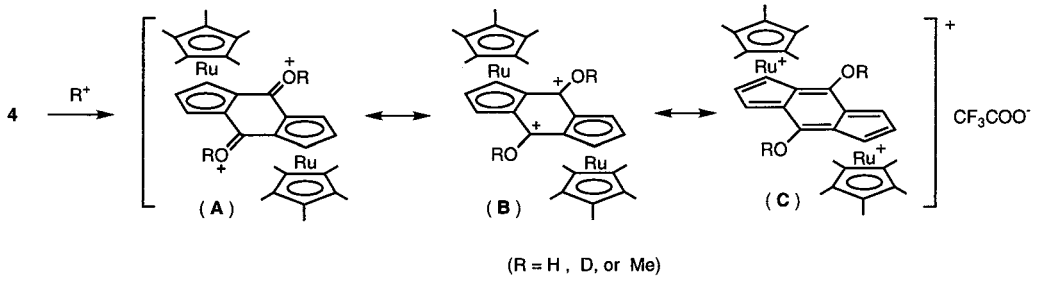

Scheme 4.

spectrum of **10** in $CDCl_3$ showed the signals of the ruthenocenyl moiety as a triplet at δ 5.48 and a doublet at δ 5.78 and the methyl signal as a singlet at δ 1.75. The spectrum is very similar to that of **4** in CF_3COOD. The ring protons of ruthenoceny moiety of **10** shifted down-field by ca. 0.75 ppm compared with that of **4**. This supports the structure doubly protonated to **4**. The single-crystal X-ray diffraction of **10** was possible only by using the crystals coated with epoxy resin, because the crystals turned back to **4** on the exposure to the air if they are not coated. Half of the molecules of **10** are crystallographically unique, with the whole molecule located on an inversion center. The crystallographic data are summarized in Table 1 and the ORTEP view of **10** is shown in Fig. 3. The selected bond distances and angles are summarized in Table 4. The central indacene framework is planar and nearly remains unchanged after protonation. The C(3)–O(2) distance [1.266(5) Å] is elongated compared with the corresponding C–O distance [1.232(6) Å] of **4**, while the C(3)–C(8) distance [1.441(5) Å] is shortened than that [1.460(7) Å] of **4**, although, the C(3)–C(4) distance is 1.480(5), meaning the weak protonation on the oxygen atom of the neutral compound **4**. On addition, the presence of the intramolecular hydrogen bond may be suggested, the distances between the O(2) atom of the central ligand and the O(3) and O(4) atoms of CF_3COO^- anion in **10** are 2.549(10) and 3.17(3) Å, respectively. The distances are somewhat longer than those of the intramolecular hydrogen bond observed in maleic acid [2.75 and 2.44 Å] [15]. These data seem to suggest that in **10** the proton weakly attaches to the oxygen atom and the carbonyl group remains its original character (**D** or **E** in Scheme 5), that is, the carbonyl group is not completely converted to the hydroxyl group (**F**). This may be supported from the fact that the C(20)–O(3) [1.10 (3) Å] and C(20)–O(4) distances [1.27(3) Å] are not equal, although, the detailed discussion is not possible, because of $R = 0.80$ and the large disorder.

The reaction of **4** with $CF_3SO_3CH_3$ gave the methylated compound **11**, *anti*-8,9,10,11,12,20,21,22,23,24-decamethyl-1,13-dimethoxy[1.1](2,15)(6,14)ruthenocenophane bis(trifluorosulfonate), in moderate yield (Scheme 4). In the ^{1}H-NMR spectrum of **11**, the ring protons of the indacene ligand appeared one triplet (2H) at δ 5.16 and one doublet (1H) at δ 5.53 and the singlet (6H) due to the methoxyl group was observed at δ 4.22, supporting the dicationic structure of **11**. However, the down-field shift ($\Delta\delta$ 0.44 and 0.51) of the former signals, compared with the corresponding protons of the neutral **4**, is considerably smaller than those of the protonated species **10** ($\Delta\delta$ 0.76 and 0.76). This seems to be attributed to the electron-releasing effect of the methyl group. In compound **4**, each one of the

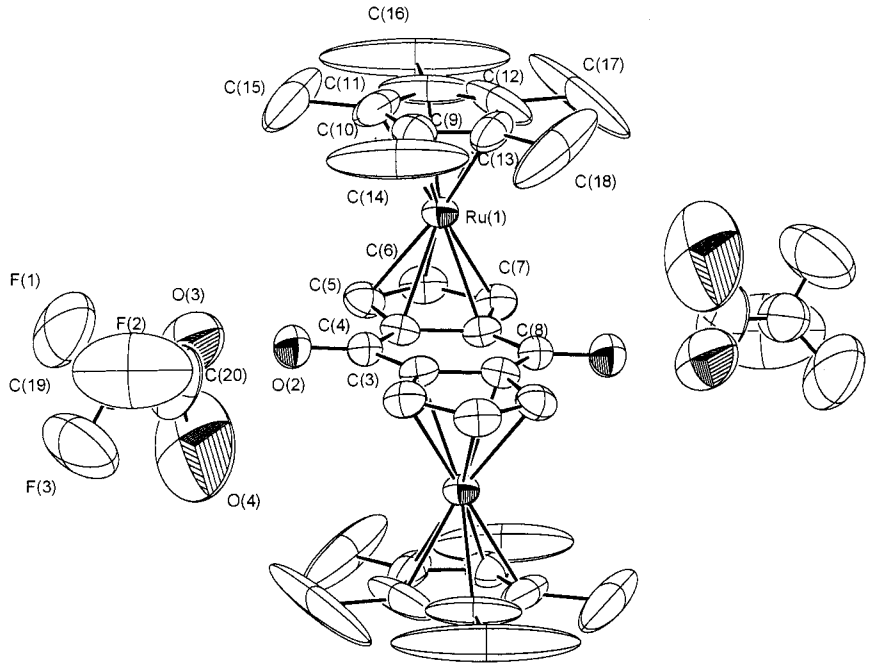

Fig. 3. ORTEP view of complex **10**.

methyl groups of the two η-C_5Me_5 ligands in the pentamethylruthenocenyl moiety are arranged above and below the plane of the carbonyl groups, so that **4** never reacted with $LiAlH_4$ or $LiAlH_4$–$AlCl_3$ in which hydride anion attacked the carbonyl group from the top and bottom of the plane. On the other hand, protonation and methylation were possible, because proton and methyl cation attacked the carbonyl group within the plane in these reactions without the steric hindrance by the methyl group.

3. Experimental

All reactions were carried out under an atmosphere of N_2 and/or Ar and workups were performed without precaution to exclude air. NMR spectra were recorded on Bruker AM400 or ARX400 spectrometer. IR (KBr disc) spectra were recorded on Perkin–Elmer System 2000 spectrometer. CV was carried out by using ALS 600 in 10^{-1} M solution of *n*-Bu_4NClO_4 (polarography grade, Nacalai tesque) in CH_2Cl_2. CV's cells were fitted with glassy carbon (GC) working electrode, Pt wire counter electrode and Ag/Ag^+ pseudo reference electrode. The cyclic voltammograms were obtained at the scan rate of 0.1 V s^{-1} in the 10^{-3} M or saturated solution of complexes. All potentials were represented versus FcH/FcH^+, which were obtained by the subsequent measurement of ferrocene at the same conditions. Solvents were purified by distillation from the drying agent prior to use as follows: CH_2Cl_2 ($CaCl_2$); $ClCH_2CH_2Cl$ ($CaCl_2$); CH_3CN (CaH_2); acetone ($CaSO_4$); THF (Na-benzophenone); ether ($LiAlH_4$). Ruthenocene [16] and 1,2,3,4,5-pentamethylruthenocene (**1**) [17] were prepared according to the literatures. Other reagents were used as received from commercial suppliers.

3.1. 1-Methoxycarbonyl-1′,2′,3′,4′,5′-pentamethylruthenocene (2)

A mixture of activated manganese oxide (Aldrich) (3.1 g, 36 mmol), potassium cyanide (0.45 g, 7 mmol), MeOH (45 ml), and AcOH (0.15 ml) was stirred for a little while under Ar. To the solution was added a solution of 1-formyl-1′,2′,3′,4′,5′ pentamethylruthenocene (**1**) (0.90 g, 2.7 mmol) in MeOH (4.5 ml) and then the mixture was stirred for 4 days at room temperature (r.t.). After filtration, the residue was washed with benzene. The filtrate and the washing were combined and evaporated under reduced pressure. The residue was chromatographed on alumina with elution

Table 4
Selected bond distances and bond angles for **10**

Bond distances (Å)			
C(3)–C(4)	1.480(5)	C(3)–C(8)	1.441(5)
C(3)–O(2)	1.266(5)	Ru(1)–C(Cp)	2.175(av.)
Ru(1)–C(Cp*)	2.144(av.)	C–C(Cp)	1.419(av.)
C–C(Cp*)	1.359(av.)		
Bond angles (°)			
C(4)–C(3)–C(8)	114.8(3)	O(2)–C(3)–C(4)	120.4(4)
O(2)–C(3)–C(8)	124.7(4)	C(3)–C(4)–C(5)	129.0(4)
C(3)–C(4)–C(8)	122.1(4)	C(5)–C(4)–C(8)	108.6(3)

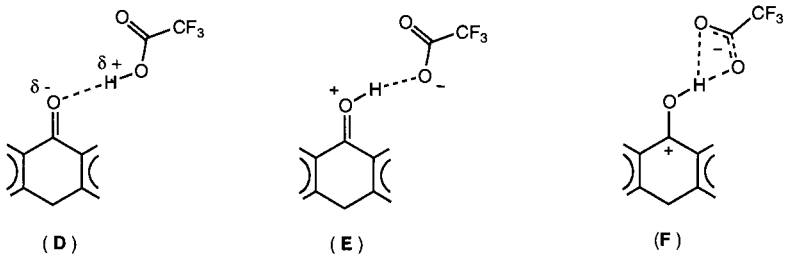

Scheme 5.

of benzene to give the title compound (0.80 g, 83% as yellow crystals. Melting point (m.p.) 72–73 °C. Anal. Found: C, 57.06; H, 6.20. $C_{17}H_{22}O_2Ru$. Calc. C, 56.81; H, 6.17%. IR (KBr): 1715 cm^{-1} (CO). ^{1}H-NMR (400 MHz, $CDCl_3$): δ 1.85 (s, 15H), 3.74 (s, 3H), 4.37 (t, $J = 1.8$ Hz, 2H), and 4.70 (t, $J = 1.8$ Hz, 2H). ^{13}C-NMR (100 MHz, $CDCl_3$): δ 11.32 (Me), 51.09 (OMe), 73.46 (η-C_5H_5), 75.43 (η-C_5H_4), 75.44 (η-C_5H_4), 76.16 (*ipso*-C_5H_4), 86.21 (*ipso*-C_5Me_5) and 169.70 (CO).

3.2. 1-Carboxy-1′,2′,3′,4′,5′-pentamethylruthenocene (3)

A mixture of **2** (1.10 g, 3 mmol), 2 M aq. NaOH solution (15 ml), and EtOH (25 ml) was refluxed under an atmosphere of nitrogen. After cooling, the mixture was poured into 1 N aq. HCl solution (100 ml). The resulting precipitate was filtered and dried to give the title compound (1.05 g, quantitative yield) as colorless solid, which was recrystallized from ethanol to give pale yellow crystals. M.p. 218 °C. Anal. Found: C, 55.62; H, 5.80. $C_{16}H_{20}O_2Ru$. Calc. C, 55.64; H, 5.84%. IR (KBr): 3200–2200 (broad) and 1682 cm^{-1}. ^{1}H-NMR (400 MHz, $CDCl_3$): δ 1.86 (s, 15H), 4.43 (t, $J = 1.8$ Hz, 2H), 4.73 (t, $J = 1.8$ Hz, 2H), and 12.06 (broad s, 1H). ^{13}C-NMR (100 MHz, $CDCl_3$): δ 10.08 (Me), 73.84 (η-C_5H_5), 75.90 (η-C_5H_4), 75.09 (*ipso*-C_5H_4), 86.27 (*ipso*-C_5Me_5) and 175.51 (CO).

3.3. anti-8,9,10,11,12,-20,21,22,23,24-decaMethyl-[1.1](2,18)(6,14)ruthenocenophan-1,13-dione (4)

A solution of **3** (100 mg, 0.30 mmol) in trifluoroacetic anhydride (2.0 ml) was heated at 85–90 °C in a sealed tube for 18 h. After cooling, the black content was washed out with CH_2Cl_2 and the washing was poured into saturated aq. Na_2CO_3 solution. The mixture was stirred for a while. The organic layer was separated, washed with water, and dried over $MgSO_4$. After evaporation, the residue was chromatographed on alumina by elution of CH_2Cl_2 to give the title compound (51 mg, 52%) as yellow crystals (m.p. > 250 °C). Anal. Found: C, 58.62; H, 5.49. $C_{32}H_{36}O_2Ru_2$. Calc. C, 58.70; H, 5.54%. IR (KBr): 1645 cm^{-1}. UV–vis (CH_2Cl_2): 403.5 (ε 9000), 315.5 (12 000), and 270.5 nm (32 000). UV–vis (60% H_2SO_4): 554 (ε 8700), 444 (10 800), 389.5 (19 000), and 282 nm (20 000). ^{1}H-NMR (400 MHz, $CDCl_3$): δ 1.66 (s, 30H, η-C_5H_5), 4.72 (t, $J = 2.5$ Hz, 2H, η-C_5H_3-β), and 5.02 (d, $J = 2.5$ Hz, 4H, η-C_5H_3-α). ^{1}H-NMR (400 MHz, CF_3CO_2D): δ 1.75 (s, 30H, η-C_5H_5), 5.49 (bs, 2H, η-C_5H_3-β), and 5.79 (bs, 4H, η-C5H3-α). ^{13}C-NMR (100 MHz, $CDCl_3$): δ 10.23 (Me), 73.42 (η-C_5H_3), 78.89 (η-C_5H_3), 83.93 (*ipso*-C_5H_3), 88.02 (*ipso*-C_5Me_5) and 187.43 (CO). ^{13}C-NMR (100 MHz, CF_3CO_2D): δ 10.54 (Me), 79.16 (η-C_5H_3), 84.70 (η-C_5H_3), 89.02 (η-C_5H_3), 96.54 (*ipso*-C_5Me_5) and 185.78 (CO).

3.4. Ethoxycarbonylruthenocene (5)

To a solution of ruthenocene (1.28 g, 5.6 mmol) in anhydrous THF (30 ml) was slowly added a solution of *t*-BuLi in pentane (4 ml of 1.5 M solution, 6 mmol) at 0 °C under Ar. The solution was stirred for 50 min and then chilled below -78 °C. To the solution was added ethyl chloroformate (0.54 ml, 5.6 mmol). The solution was warmed gradually to r.t. and then stirred overnight. After the solvent was evaporated under vacuum, the residue was dissolved in CH_2Cl_2 and water. The organic layer was separated and the aqueous (aq.) layer was extracted with CH_2Cl_2. The organic layer and the extracts were combined and then dried over $MgSO_4$. After the solvent was evaporated under vacuum, the residue was chromatographed on Al_2O_3 to give ruthenocene (0.56 g, 44%), Ethoxycarbonylruthenocene (**5**) (0.75 g, 44%), and 1,1′-bis(ethoxycarbonyl)ruthenocene (0.16 g, 8%).

5: M.p. 80–81 °C. Anal. Found: C, 51.75; H, 4.59. $C_{13}H_{14}O_2Ru$. Calc.: C, 51.48; H, 4.65%. IR (KBr): 1683 cm^{-1} (ν_{CO}). ^{1}H-NMR (400 MHz, $CDCl_3$): δ 1.28 (t, $J = 7.4$ Hz, 3H, CH_3), 4.18 (q, $J = 7.4$ Hz, 2H, CH_2), 4.58 (s, 5H, η-C_5H_5), 4.69 (t, $J = 1.5$ Hz, 2H, η-C_5HO), and 5.13 (t, $J = 1.5$ Hz, 2H, η-C_5H_4-α). ^{13}C-NMR (100 MHz, $CDCl_3$): δ 14.34 (CH_3), 60.04 (CH_2), 71.61 (η-C_5H_4-β), 71.72 (η-C_5H_5), 72.71 (η-C_5H_4-α), 75.89 (η-C_5H_4-*ipso*), and 170.25 (CO).

1.1′-Bis(ethoxycarbonyl)ruthenocene: m.p. 89–90 °C. Anal. Found: C, 51.38; H, 4.72. $C_{16}H_{18}O_4Ru$. Calc.: C, 51.19; H, 4.83%. IR (KBr): 1683 cm^{-1} (ν_{CO}). ^{1}H-NMR (400 MHz, $CDCl_3$): δ 1.30 (t, $J = 7.1$ Hz, 3H, CH_3), 4.21 (q, $J = 7.1$ Hz, 2H, CH_2), 4.58 (s, 5H,

η-C_5H_5), 4.72 (t, $J = 1.7$ Hz, 2H, η-C_5H_4-β), and 5.16 (t, $J = 1.7$ Hz, 2H, η-C_5H_4-α). ^{13}C-NMR (100 MHz, $CDCl_3$): δ 14.32 (CH_3), 60.31 (CH_2), 73.20 (η-C_5H_4-β), 74.20 (η-C_5H_4-α), 77.49 (η-C_5H_4-*ipso*), and 169.07 (CO).

3.5. anti-[1.1](2,18)(6,74)Ruthenocenophan-1,13-dione (8) and [1,1](2,20)(8,14)ruthenocenophane-1,13-dione (9)

To a solution of chlorocarbonylruthenocene (**7**) (62 mg, 0.20 mmol) in dichloroethane (10 ml) was added aluminum chloride (52 mg, 0.39 mmol). The mixture was refluxed for 12 h under N. After being hydrolyzed with water, the mixture was extracted with CH_2Cl_2. A large amount of the decomposed products were seen. The extract was dried over $MgSO_4$ and evaporated in vacuum. The residue was chromatographed on SiO_2 with benzene–EtOAc to give diketones **8** (1.5 mg, 3%) and **9** (1.5 mg, 3%), along with a complex mixture. No starting material could be found.

Compound **8**: m.p. > 250 °C. Anal. Found: C, 51.69; H, 2.99. $C_{22}H_{16}O_2Ru_2$. Calc.: C, 51.36; H, 3.13%. UV–vis (CH_2Cl_2): 386 (ε 6000), and 255.5 nm (38 000). UV–vis (60% H_2SO_4): 533.5 (ε 900), 378 (6800), and 280 nm (11 200). ^{1}H-NMR (400 MHz, $CDCl_3$): δ 4.62 (s, 10H, η-C_5H_5), 5.01 (t, $J = 2.6$ Hz, η-C_5H_3-β), and 5.48 (d, $J = 2.6$ Hz, η-C_5H_3-α). ^{1}H-NMR (400 MHz, CF_3CO_2D): δ 4.93 (s, 10H, η-C_5H_5), 5.63 (bs, 2H, η-C_5H_3-β), and 6.04 (bs, 4H, η-C_5H_3-α). ^{13}C-NMR (100 MHz, $CDCl_3$): δ 71.69 (η-C_5H_4-β), 74.60 (η-C_5H_4-α), 82.83 (η-C_5H_4-*ipso*), and 190.34 (CO).

Compound **9**: m.p. > 250 °C. Anal. Found: C, 51.01; H, 3.00. $C_{22}H_{16}O_2Ru_2$. Calc.: C, 51.36; H, 3.13%. IR (KBr): 1627 cm^{-1} (CO). UV–vis (CH_2Cl_2): 378 (ε 1400), and 265 mm (11 200). ^{1}H-NMR (400 MHz, $CDCl_3$, r.t.): δ 4.77 (bs, η-C_5H_3-β), and 5.48 (bs, η-C_5H_3-α). ^{1}H-NMR (400 MHz, $CDCl_3$, 333 K): δ 4.76 (t, $J = 2.6$ Hz, η-C_5H_3-β), and 5.47 (t, $J = 2.6$ Hz, η-C_5H_3-α). ^{1}H-NMR (400 MHz, $CDCl_3$, 223 K): δ 4.72 (bt, η-C_5H_3-α), 4.90 (bt, η-C_5H_3-β) 5.46 (bs, η-C_5H_3-β), and 5.58 (bs, η-C_5H_3-α). ^{13}C-NMR (100 MHz, $CDCl_3$): δ 71.69 (η-C_5H_4-α), 74.60 (η-C_5H_4-α), 82.83 (η-C_5H_4-*ipso*), and 190.34 (CO).

Compound **8** was also prepared in a trace yield by using the procedure described above about the preparation of **4**.

3.6. Protonation of 4

A solution of **4** (10 mg, 0.015 mmol) in trifluoroacetic acid (ca. 0.5 ml) was stirred for 3 h under nitrogen. After the solution had been condensed under reduced pressure, the solution of the residue in a small amount of benzene was diffused with pentane in the refrigerator. The hygroscopic red crystals were isolated. ^{1}H-NMR ($CDCl_3$): δ 1.75 (s, 30H, Me), 5.48 (t, $J = 2.9$ Hz, 2H, β-H), and 5.78 (d, $J = 2.9$ Hz, 4H, α-H).

3.7. Methylation of 4

A solution of **4** (52 mg, 0.078 mmol) in methyl trifluorosulfonate (ca. 2 ml) was stirred for 3 h under nitrogen. After evaporating under reduced pressure, the solution of the residue in a small amount of benzene was diffused with pentane in the refrigerator. The hygroscopic and dark red crystals were isolated. ^{1}H-NMR ($CDCl_3$): δ 1.66 (s, 30H, Me), 4.22 (s, 6H, Me), 5.16 (t, $J = 2.9$ Hz, 2H, β-H), and 5.53 (d, $J = 2.9$ Hz, 4H, α-H).

3.8. Structure determinations

The crystallographic data are listed in Table 1 for **4**, and **10**. Data collections for **10** were performed at r.t. on Mac Science MXC18K diffractometer with graphite monochromated Mo–K_α radiation and an 18-kW rotating anode generator. The structure was solved with the Diadif–Patty or SIR method in CRYSTAN-G (software-package for structure determination) and refined by full-matrix least-squares procedure. Absorption correction with the Ψ-scan method and anisotropical refinement for non-hydrogen atom was carried out. Data collections of crystal data for **4** were performed at r.t. by the Weissenberg method on Mac Science DIP3000 image processor with graphite monochromated Mo–K_α radiation and an 18-kW rotating anode generator. The structure was solved with the SIR method in MAXUS (software-package for structure determination) and refined finally by full-matrix least-squares procedure. Absorption correction with the Sortav method and anisotropical refinement for non-hydrogen atom was carried out. All the hydrogen atoms, located from difference Fourier maps, were isotopically refined.

4. Supplementary material

Crystallographic data for the structural analysis have been deposited with the Cambridge Crystallographic Centre, CCDC no. 170610 for complex **4** and CCDC no. 170611 for complex **10**. Copies of this information may be obtained free of charge from: The Director, CCDC, 12 Union Road, Cambridge DB2 1EZ, UK (Fax: +441223-336-033; e-mail: deposit@ccdc.cam.ac.uk or www:http://www.ccdc.cam.ac.uk).

Acknowledgements

The present work was supported by a Grant-in Aid for Science Research (No. 10640538) from the Ministry of Education, Science, and Culture of Japan.

References

[1] (a) G Wilkinson, F.G.A. Stone, E.W. Abel (Eds.), Comprehensive Organometallic Chemistry, vol. 4, Oxford Pergamon, 1982, pp. 377, 691, and 967;
(b) Comprehensive Organometallic Chemistry II, Pergamon New York, 1995.
[2] A. Togni, T. Hayashi, Ferrocenes, VCH, New York, 1995.
[3] U.T. Mueller-Westerhoff, A.L. Rheingold, G.F. Swiegers, Angew. Chem. Int. Ed. Engl. 31 (1992) 1352.
[4] (a) M. Sato, A. Kudo, Y. Kawata, H. Saitoh, J. Chem. Soc. Chem. Commun. (1996) 25;
(b) M. Sato, Y. Kawata, A. Kudo, A Iwai, H Saitoh, S. Ochiai, J. Chem. Soc. Dalton Trans. (1998) 2215.
[5] M. Sato, Y. Kawata, H. Shintate, Y. Habata, S. Akabori, K. Unoura, Organometallics 16 (1997) 1693.
[6] M. Sato, A. Iwai, M. Watanabe, Organometallics 18 (1999) 3208.
[7] M. Watanabe, M. Sato, T. Takayama, Organometallics 18 (1999) 820.
[8] M. Sato, M. Asai, J. Organomet. Chem. 430 (1992) 105.
[9] M. Watanabe, M. Sato, A. Nagasawa, I. Motoyama, T. Takayama, Bull. Chem. Soc. Jpn. 71 (1998) 2127.
[10] U.T. Mueller-Westerhoff, Angew. Chem. Int. Ed. Engl. 25 (1986) 702.
[11] W.E. Watts, J. Organomet. Chem. Lib. 7 (1979) 399.
[12] J. Kotz, D. Pedrotty, Organometal. Chem. Rev. (A) 4 (1969) 479.
[13] M. Sato, Y. Kawata, H. Shintate, Y. Habata, S. Akabori, K. Unoura, Organometallics 16 (1997) 1693.
[14] M. Sato, Y. Kawata, in preparation.
[15] H.M.E. Cardwell, J.D. Dunitz, L.E. Orgel, J. Chem. Soc. (1953) 3740.
[16] P. Pertici, G. Vitulli, M. Paci, J. Chem. Soc. Dalton (1980) 1961.
[17] A.R. Kudinov, M.I. Rybinskaya, Y.T. Struchkov, A.I. Yanovskii, P.V. Petrovskii, J. Organomet. Chem. 336 (1987) 187.